Wind Forces in Overgrown Rope Façades

Drag Coefficient Suggestion for Climbing Plants Based on Study Review

Kilian Arnold*, Susanne Gosztonyi, Andreas Luible

* Corresponding author
Lucerne University of Applied Sciences and Arts Engineering and Architecture, kilian.arnold@hslu.ch

Abstract

Modern cities face a climatic problem due to the high proportion of sealed surfaces that increase the urban heat island (UHI) effect. Green surfaces offer a way to mitigate the UHI effect, as they positively influence the thermal energy storage and air temperature. To support an increase of green surfaces in the limited resources of cities, vertical spaces, e.g. façades, must be exploited. A possible realisation of a vertical green system are overgrown rope façades. Overgrown rope façades have pre-fitted ropes in front of façades on which climbing plants can grow. However, such systems have to deal with dynamic wind forces, which pose static challenges to the climbing system. In order to design such systems for the effective wind forces, so-called drag coefficients of the climbing plants must be known. Unfortunately, there are no guidelines or known values that provide such specific drag coefficients for climbing plants. In this study, based on a study review of relevant data for drag coefficients on deciduous and coniferous trees and leaves, findings are made comparable by applying the power function. Six critical factors to be considered are identified and a drag coefficient for climbing plants is derived from the investigations on deciduous trees. Their transferability to overgrown rope façades is analysed and discussed.

Keywords

Green façades, wind forces, overgrown rope façades, drag coefficient, climbing plants, urban greenery, UHI, vertical green systems

10.7480/jfde.2021.2.4831

1 INTRODUCTION

In the year 2050, 66% of the global population will live in cities, thereby inhabiting 3% of the earth's surface and consuming 60% to 80% of worldwide energy (Leal Filho et al., 2017). Due to the large share of sealed surfaces in cities and the related increase in the heat storage capacity of the surfaces, cities are heating up at a faster pace than rural areas (Mohajerani et al., 2018). This phenomenon is known as urban heat island (UHI) effect (Gartland, 2012). Available data show that cities are heating up due to the UHI by up to 10°C over the average temperature compared to rural zones (Santamouris et al., 2001). A promising approach for mitigating the UHI problem involves increased usage of horizontal and vertical green spaces in cities (Kolokotsa et al., 2013). Vertical green systems can contribute to the decrease of urban temperatures more effectively than roof greening because they influence the thermal absorption of ground level directly, which affects the urban heat island effect, thermal comfort, and building cooling demand substantially more than rooftops facing to the sky (Djedjig et al., 2015; Alexandri & Jones, 2008). For vertical green systems, three further greening approaches exist besides ground-based (direct) vegetation (e.g. ivy) (1); "Overgrown rope façades" (2); "balcony boxes greening systems" (3); and "Living wall" - wall-based surface greening (4), (Pfoser, 2016)(see Figure 1).

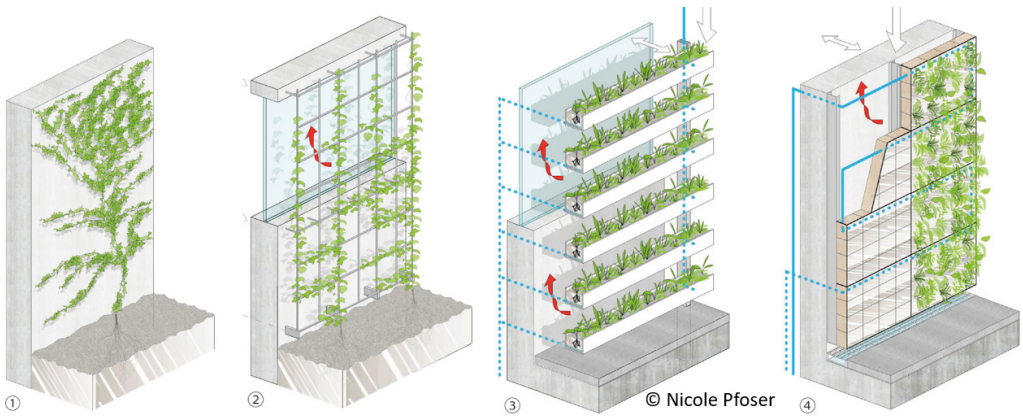

FIG. 1 Different vertical green systems: 1) ground-based; 2) overgrown rope façades; 3) balcony boxes system; 4) living wall. (Pfoser, 2016, p. 126/127, fig. 137) & (Pfoser, 2018, p. 166-167)

This paper focusses on the type "overgrown rope façades" since this vertical greening system belongs to the category of wind flow-through systems. Compared to typical vertical green systems their spans of climbing systems with ropes are larger and consequently the forces acting on the building structure are higher. Ropes have no inherent rigidity, which means that the wind forces are transferred via tensile forces in the ropes, resulting in very high anchorage loads (Meskouris et al., 2012). A climbing aid based on rope constructions is provided in front of façades that allows growth heights of the climbing plants, rooted in the ground, of up to 30m (Pfoser, 2016). These climbing systems must be able to bear forces including the wind forces acting upon the plants. In order to determine these wind forces for moving in flow bodies and thus correctly design these systems according to the respective building standards, such as e.g. the Swiss standard (SIA 261, 2014) or European standard (EN 1991-1-4, 2010), so-called drag coefficients C_D are required, which have to be calculated as:

$$F_w = c_D \cdot A \cdot \frac{\rho \cdot v^2}{2} \text{ [N]} \tag{1.1}$$

Where F_W is the wind force, C_D the drag coefficient, A the projection area, ρ the density, and v the flow speed of the medium. For the calculation of wind forces associated with simple geometries of rigid bodies, suitable drag coefficients can be found in the respective standards for flow force determination. The wind speeds on a building are dependent on the building site as well as the building shape. Thus, different speeds arise for different buildings.

The research questions discussed in this article are as follows: What is the interaction between the speed of the wind and the resulting force? Can the wind force of the climbing plants of overgrown rope façades in the wind flow be calculated by formula (1.1)? If so, what are the drag coefficients of climbers and how do they behave with increasing speed?

It is important to determine the correct loads for the climbing systems of overgrown rope façades. The resulting higher loads lead to uneconomic anchorage systems and load bearing structures as well as higher material consumption, thereby entailing aesthetic compromises as well as higher building costs. These factors contribute to lower acceptance of the use of overgrown rope façades in practical implementations.

In Section 2, the results of a comprehensive literature search are presented, which involves the identification and examination of study data related particularly to drag coefficients of plants. In connection to the data identification, basic rules are presented that contain statements about wind load reductions for overgrown rope façades. In Section 3, the data findings are analysed based on a comparative analysis methodology. Tables with comparable drag coefficients of coniferous and deciduous trees as well as individual leaves and clusters are established. Section 4 focuses on the discussion of the data and approaches in order to identify and apply the critical parameters for an appropriate calculation model. This model envisages six influencing factors and is suggested to enable calculation of dynamic wind forces on overgrown rope façades. The model is developed based on the analysed data. Finally, a drag coefficient is suggested as a hypothesis for climbing plants on overgrown rope façades in Section 5.

2 DATA REVIEW

A literature review has been conducted to get an overview of peer-reviewed articles and guidelines, initially linked to the keywords “wind” AND “climbing plants” or “vertical green systems.” Further keyword combinations have been added, such as “wind loads” AND “plants,” “trees,” as well as “drag coefficient” AND “plants,” “leaves,” “trees,” and finally also “cd value” AND “plants” to refine the results towards wind dimensioning issues. This approach has led to 58 publications, of which only nine deal specifically with wind forces on plants. Most of the publications identified in this search deal with the interrelation between wind and plants without providing insights into specific dimensioning parameters, such as the drag coefficient. The search was done in electronic databases of ScienceDirect and GoogleScholar.

The most relevant articles and publications, which are listed in Table 1, are examined in more detail in order to understand and compare the approaches for assessing wind forces on plants. The findings of this review are presented in brief in the following subsections, 2.1 to 2.4, and analysed in Section 3.

TABLE 1 Relevant publications

#	AUTHOR(S)	MAIN FOCUS AND CHALLENGES	PUBLICATION TYPE	REF. TO SUBSEC.
1	Mayhead, 1973	Drag coefficients for forest trees (fir), Size of samples, wind tunnel testing	Scientific article	2.1
2	Rudnicki et al., 2004	Static and dynamic drag coefficients for forest trees (fir) over the projection area, wind tunnel testing	Scientific article	2.1
3	Vollsinger et al., 2005	Static and dynamic drag coefficients for forest deciduous trees over the projection area, wind tunnel testing	Scientific article	2.2
4	Kane & Smiley, 2006	Drag coefficients for red maple, size of samples, pick-up truck testing	Scientific article	2.2
5	Koizumi et al., 2009	Drag coefficients of poplar crowns under natural condition	Scientific article	2.2
6	Vogel, 1984	Drag and flexibility in sessile organisms, E-values	Scientific article	2.3
7	Vogel, 1989	Drag coefficients for leaves and cluster of deciduous trees, E-values	Scientific article	2.3
8	Kane et al., 2008	Drag coefficients for deciduous trees, E-values, pick up testing	Scientific article	2.3
9	FLL*, 2018	Planning of façade greening systems	Planning guidelines	2.4

** Forschungsgesellschaft Landschaftsentwicklung Landschaftsbau e.V.*

2.1 DRAG COEFFICIENT OF FIR

Mayhead (1973) investigated the drag coefficients of various fir species in a wind tunnel. The samples had a height of 5.8m to 8.5m. For Mayhead (1973), it was important for the fresh samples to be as large as possible since they have a different morphology compared to small, young firs. The effective drag resistance in the airflow of the wind tunnel was measured in the speed range from 9.1m/s to 26.5m/s. The crown area of the samples was determined in still air based on photographs. Mayhead (1973) calculates the resistance forces according to formula (1.1) and characterised the course of the drag coefficient C_D using a polynomial function according to formula.

$$c_D = a + b \cdot v + c \cdot v^2 \text{ [-]} \tag{2.1}$$

Where v is the flow speed, and a,b and c are plant-specific constants.

The drag coefficients calculated from the resistance measurements were determined at various measured speeds. Based on the experimental data, Mayhead (1973) subsequently determined critical drag coefficients using extrapolations that can be applied in the calculation of critical tree heights (Table 2).

TABLE 2 Values of drag coefficient for use in critical height determinations. Extract from (Mayhead, 1973, p. 129, Table III)

SPECIES	DRAG COEFFICIENT	SPECIES	DRAG COEFFICIENT
Grand fir	0.36	Scots pine	0.29
Sitka spruce	0.35	Douglas fir	0.22
Norway spruce	0.35	Lodgepole pine	0.20
Corsican pine	0.32	Western hemlock	0.14

In contrast, Rudnicki et al. (2004) investigated three different coniferous species in terms of how the different projection area in the flow impacts the drag coefficient. The investigated coniferous species had heights ranging from 2.5m to 5m, but had to be trimmed to the wind tunnel height of 1.9m. They measured the drag resistances in the flow at speeds of 4, 8, 12, 16, and 20m/s at intervals of 30 seconds. The classic formula in this study for wind drag is again the formula (1.1). The measured data were evaluated based on two different models: The static model is based on determination of the projection area of the samples in the stationary state, whereby the drag coefficient is always referenced to the stationary projection area. The dynamic model is based on the variable projection area at different flow speeds, whereby the drag coefficient is referenced to the variable projection area at each measurement speed. The drag coefficients of the static model at 20m/s are shown in Table 3.

TABLE 3 Values of drag coefficient. Extract from (Rudnicki et al., 2004, p. 670, Fig.2)

SPECIES	SPEED [m/s]	DRAG COEFFICIENT
Red cedar	20	0.2
Hemlock	20	0.53
Lodgepole pine	20	0.47

2.2 DRAG COEFFICIENTS OF DECIDUOUS TREES

As in the study by Rudnicki et al. (2004), Vollsinger et al. (2005) performed tests on deciduous trees in a comparable wind tunnel setting. The classic formula for calculating wind drag is again formula (1.1). They also compared the static model for the drag coefficient with the dynamic model. The samples were 3m to 5m in size and were trimmed to a height of 1.9m for the analysis due to the limited wind tunnel size. They measured the drag resistances in the flow at the same speeds of 4, 8, 12, 16, and 20m/s at 30 second intervals, like in the above presented study. Again, the drag coefficients of the static model at 20m/s are shown in Table 4.

TABLE 4 Values of drag coefficient. Extract from Vollsinger et al (2005, p. 1243).

SPECIES	SPEED [m/s]	DRAG COEFFICIENT
Paper birch	20	0.15
Black cottonwood	20	0.17
Red alder	20	0.22
Big leaf maple	20	0.26
Quaking aspen	20	0.28

In order to allow testing of larger samples, Kane and Smiley (2006), in another study on deciduous trees, mounted 80 red maple trees with a height of 2.7 – 5.1m on a pickup truck for the purpose of driving over a straight course with the samples. The test course was driven in both directions in order to take the average value of the measurements in both directions. They only performed tests on calm days with wind speeds of less than 2m/s. The projection area of the samples was determined in the stationary state using graphics software (Photoshop). The drag coefficient was calculated based

on the force measurements in the ropes, the speed measurement above the pickup truck and the determined projection area. The pickup truck accelerated from 0 to 20m/s, whereby the force values were determined at speeds of 11, 16. and 20m/s. The force F in [N] (average value) for the 5m tall red maple samples was calculated according to formula (2.2), in which the force is proportional to the speed to a power of 1.4 ($F \propto v^{1.4}$) (Kane & Smiley, 2006, p. 1953).

$$F = 7.81 \cdot v^{1.4} \text{ [N]} \tag{2.2}$$

In the third study involving deciduous trees, Koizumi et al. (2010) examined the drag coefficient on three free-standing poplar trees. By means of pull pre-tests, the deflection of the trees was determined at the effective pulling force. Based on the wind speed measurement and the deflection of the tree during the measurement duration, the effective force was extrapolated under real wind loads. They determined the drag coefficients from these force values and the photograph of the crown projection areas. In their measurements, Koizumi et al. (2010) realised wind speeds from 2 to 15m/s. The wind drag is determined by formula (1.1). The determined drag coefficients were interpolated with power functions for which the values are documented in Table 5.

TABLE 5 Drag coefficients of poplar trees. Extract from (Koizumi, Motoyama, Sawata, Sasaki, & Hirai, 2010, p. 192, Fig. 6)

POPLAR TREE	HIGH [m]	PROJECTED AREA A [m²]	FUNCTION OF DRAG COEFFICIENT C_D
Poplar tree no. 1	13.1	32.5	$Y = 1.77 \cdot X^{-0.911}$
Poplar tree no. 2	12.3	22.0	$Y = 1.14 \cdot X^{-0.824}$
Poplar tree no. 3	12.9	29.0	$Y = 1.79 \cdot X^{-0.714}$

2.3 E-VALUES FOR THE DETERMINATION OF DRAG COEFFICIENTS

The E-value is referred to as follows: "*E represents the exponent to which the speed must be raised to be directly proportional to either the drag coefficient or the drag divided by the square of speed*" (Vogel, 1989, p. 943). If the E-value in the proportion in formula (2.3) assumes a value of -2, the speed *v* is cancelled out of the equation such that the force F is no longer proportional to the speed.

$$\frac{F}{v^2} \propto v^E \tag{2.3}$$

The derivation of the E-value according to (Vogel, 1984) is stated as following: "*We're left with* formula (2.3) *as our baseline, plotting F / v² (ordinate) versus v (abscissa) and looking for deviations from horizontality. F / v² might be termed the "speed specific drag". For regions on a graph without inflection points, the exponent can be derived by a linear regression as the slope of the plot of the logarithms of F / v² an v. This slope, then, can be taken as a "figure of merit" – the lower (more negative) the value, the more noteworthy the relative reduction of drag as speed is increased; we will denote the slop or exponent as "E"*." (Vogel, 1984, p.39).

Vogel (1984) calculated the E-value based on various studies of resistance measurements on bodies and plants. The plant species were subjected to a flow comprising the medium of water or air. Selected E-values calculated by Vogel, which are relevant in connection with plants for overgrown rope façades, are documented in Table 6. Most of the tests of these selected E-values were carried out at a speed of 8 to 20 m/s.

TABLE 6 Selected E-values of different species. Extract from (Vogel, 1984, p. 40, Table 1)

SPECIES	E-VALUE	SPECIES	E-VALUE
Pinus sylvestris	-0.72	Ilex opaca, branch	-0.10
Pinus taeda, 1 m high	-1.13	Pinus taeda, control	-1.11
Ilex opaca, 1 m high	-1.30	Pinus taeda, shaken	-1.12
Pinus taeda, branch	-1.16		

A few years later, Vogel (1989) determined further drag coefficients on individual leaves and clusters of trees. The samples were mounted directly at the outlet of a chaotically turbulent airflow from a pipe. The justification for usage of a turbulent stream of air is that the leaves of the trees are exposed to a highly turbulent airflow, meaning that the drag resistances must be measured in a comparable test environment, i.e. in a turbulent airflow. The tests were performed in a speed range from 10 to 20m/s at individual speed levels of 10, 12.5, 15, 17.5, and 20m/s. In the study by Vogel (1989), the resulting drag coefficients were documented in the form of diagrams as well as calculated E-values (Table 7).

TABLE 7 Selected E-values of different species. Extract from (Vogel, 1989, p. 945, Table 2)

SPECIES	E-VALUE	SPECIES	E-VALUE
Black locust (leaf)	-0.52	Tuliptree (leaf)	-1.18
Black walnut (leaf)	-0.76	Tuliptree (cluster)	-0.91
Pignut hickory (leaflet)	-0.2	White oak (leaf)	+0.97
Pignut hickory (leaf)	-0.78	White oak (cluster)	-0.44
Red maple (leaf)	-0.79	White poplar (cluster)	-0.60
Red maple (cluster)	-0.64	Willow oak (cluster)	-1.06

Kane et al. (2008) repeated the test course of Kane & Smiley (2006) on three further tree species (Freeman maple, shingle oak, and swamp white oak) and calculated the corresponding E-values which they took over from Vogel (1984). In the acceleration of the vehicle, attention was paid starting at 11m/s to ensure that the additional effective force caused by the acceleration was linear, so that it can later be subtracted from the drag resistance of the samples. This additional force due to the acceleration is less than 2% of the drag resistance of the samples. The drag resistance F of the samples is proportional to the speed v with an approximate exponent of 1.3 ($F \propto v^{1.3}$). The drag coefficient for the studied tree species is inversely proportional to the speed and varies from species to species. The E-values determined by Kane et al. (2008) are documented in Table 8.

TABLE 8 E-values of three tree species. Extract from (Kane, Pavlis, Harris, & Seiler, 2008)

TREE SPECIES	E-VALUE
Freeman maple	-0.77
Shingle oak	-0.70
Swamp white oak	-0.80

2.4 GUIDELINES FOR GREEN FAÇADES

In contrast to the previously presented studies, the guideline set entitled "Fassadenbegrünungsrichtlinien" ("Green Façade Guidelines") (FLL, 2018) by the Forschungsgesellschaft Landschaftsentwicklung Landschaftsbau e.V., in brief FLL, provides data without any information about their development. The document contains information for wind load dimensioning for climbing plants, including reduction factors (drag coefficients). The reduction factors are based on assumptions about the throughput: *"Climbing plants are flown through by the wind in a similar way to deciduous trees, even if their foliage is arranged in shingle-like overlapping patterns and the growth is very dense. The reduction factors mentioned above take into account that stronger shoots are fixed to climbing aids or wall surfaces and that plants react therefore less elastically to wind pressure (and suction) than trees"* (FLL, 2018 p. 92). Accordingly, this guideline divides climbing plants into load classes. For each of these load classes, the reduction factors (only drag coefficients) are documented in Table 9.

TABLE 9 Reduction factors (drag coefficients) for climbing plants due to throughput. Selected value extract from: (FLL, 2018 p. 92, Table 7)

LOAD CLASS	1 VERY LIGHT	2 LIGHT	3 MEDIUM	4 HEAVY	5 VERY HEAVY
Wind loads - possible reduction due to throughput (drag coefficients)	0.55	0.6	0.6	0.65	0.7

3 ANALYSIS OF EXISTING DRAG COEFFICIENTS

Examination of the factors applied in the analysed studies are compared in subsection 3.1. In section 3.2, the mathematical approaches in the studies are reflected, and in section 3.3, a comparison basis is developed. Finally, in section 3.4 the study data is shown in comparable values and tables.

3.1 TEST VARIABLES OF THE EXAMINED STUDIES

In the examined studies, the test parameters vary. Table 10 gives an overview of the various test parameters applied in the studies. The guideline set is omitted in this comparative analysis due to its different approach and lack of comparable factors relating to the test environment.

TABLE 10 Different test parameters of the relevant studies

AUTHOR(S)	SPECIES	SIZE OF SPECIES	SIZE OF SAMPLE	HIGH OF SAMPLE [m]	TEST SPEED [m/s]	AIRFLOW	TEST METHOD
Mayhead, 1973	Fir	7	1 - 4	5.8 – 8.5	9.1 – 26.5*	laminar	Wind tunnel
Rudnicki et al., 2004	Fir	3	8	1.9	4 - 20	laminar	Wind tunnel
Vollsinger et al., 2005	D. trees	5	8	1.9	4 - 20	laminar	Wind tunnel
Kane & Smiley, 2006	Red maple	1	80	2.7 – 5.1	0 - 20	laminar	Pickup truck
Kane et al., 2008	D. trees	3	13 - 18	4.4 – 4.8 (mean)	0 – 24.5	laminar	Pickup truck
Koizumi et al., 2009	Poplar tree	1	3	12.3 – 13.1	2 - 14	turbulent	Field test
Vogel, 1989	Leaves	8	5 - 8	-	10 - 20	turbulent	Pipe

** Only one sample was tested at a speed of up to 38.3m/s*

Despite the somewhat different test environments and factors, some essential conclusions can be drawn.

3.2 METHODICAL DERIVATION OF THE MATHEMATICAL MODEL

In almost all reviewed publications of section 2, the flow forces on plants are determined according to formula (1.1), the classical formula for wind drag determination. The drag coefficient characterises the aerodynamic properties of the drag body in the flow. The more aerodynamically the flow surrounding a body behaves, the smaller the drag coefficient gets, resulting in a smaller airflow resistance force according to formula (1.1).

The proportional relationship between flow speed and force with the E-value that was examined by Vogel (1989, p. 943) is characterised in formula .

$$\frac{F_w}{v^2} \propto v^E \rightarrow F_w \propto v^2 \cdot v^E \rightarrow F_w \propto v^{2+E} \tag{3.1}$$

This proportionality formula (3.1) contains the quadratic speed term that is known from fluid dynamics according to formula (1.1). The E-value represents the deformation capacity of the plants (reduction in projection area at increasing flow speeds) according to Vogel (1984). The deformation capacity of the plants at increasing speeds can be characterised by a potential course of the drag coefficient C_D, whereby the proportion from formula (3.1) can be applied to the drag coefficient according to formula (3.2).

$$c_D \propto v^E \tag{3.2}$$

By inserting the proportion constant B (B-value) of the power function, the proportionality symbol in formula (3.2) is replaced by an equals sign, thereby yielding formula (3.3). Alongside the E-value, the B-value is a second constant of the power function that characterises the drag coefficient versus speed.

$$c_D = B \cdot v^E \text{ [-]} \tag{3.3}$$

By combining formula (3.3) with formula (1.1), formula (3.4) is obtained. This formula can also be derived by adding the proportion constant $\frac{B \cdot A \cdot \rho}{2}$ into formula (3.1).

$$F_w = B \cdot v^E \cdot A \cdot \frac{\rho \cdot v^2}{2} = B \cdot A \cdot \frac{\rho \cdot v^{2+E}}{2} \text{ [N]} \tag{3.4}$$

Formula (3.4) shows that the wind force does not increase proportionally to the wind speed on a quadratic basis (as is usual) and that the increasing porosity of the plants is taken into account at increasing speeds by the E-values.

3.3 DETERMINATION OF COMPARISON VALUES FOR THE ANALYSIS

Due to the difficulty of comparing the different study results and values documented in section 2, it is necessary to prepare the data for a comparative analysis. Thus, the function values for the drag coefficients are determined by interpolating the various study data on the drag coefficients with the least squares method and specification of the function course according to formula (3.3). In cases where no numerical values are documented for the drag coefficients in the studies, individual data points are deduced from the curve progressions of the drag coefficients at different speeds. The quality of the interpolated curve is calculated based on the coefficient of determination R^2. The coefficient of determination R^2 indicates the extent to which the interpolated function follows the extracted data points. A function with a determination close to 1 perfectly follows the data points, whereas a function with a determination close to 0 does not follow the data pints. Figure. 2 shows an example for an interpolation of the data points of drag coefficients for Scots pine.

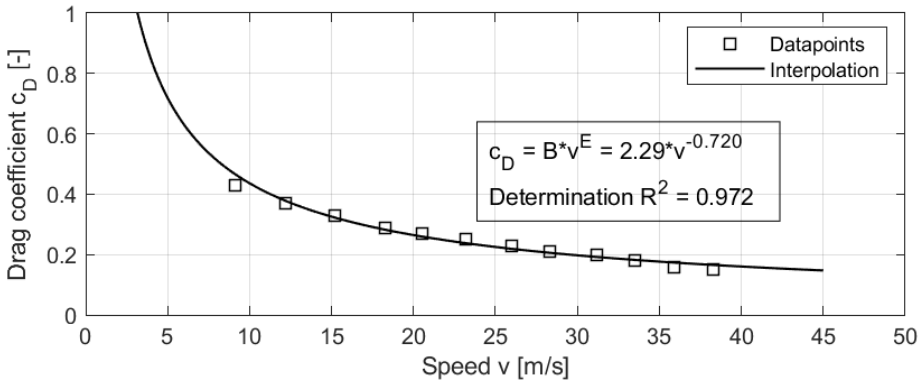

FIG. 2 Interpolation of data points for Scots pine, source of the data by (Mayhead, 1973)

The obtained functions can thus be compared based on the B-value and E-value parameters. To ensure that the functions remain comparable in terms of the magnitude, the function value is specifcoefficients

3.4 ANALYSIS OF THE DRAG COEFFICIENTS

Based on the preparation for the comparison of the various data, as described in subsection 3.3, the results of the examined studies are presented in an adapted comparative form, arranged by the static and dynamic models and by coniferous and deciduous tree species, as well as individual leaves and clusters of deciduous trees.

3.4.1 Drag Coefficients For Coniferous Trees

The analysis results for the drag coefficients for a static projection area (applying the static model) in different coniferous tree species are documented in Table 11.

TABLE 11 Drag coefficient of the static projection area of fir

FIR	B-VALUE	E-VALUE	C_D	C_D [v=20m/s]	R^2	SOURCE
Corsican Pine 1	3.88	-0.68	$3.88 \cdot v^{-0.68}$	0.51	0.995	Mayhead, 1973
Corsican Pine 2	3.23	-0.68	$3.23 \cdot v^{-0.68}$	0.43	0.998	Mayhead, 1973
Corsican Pine 3	2.45	-0.60	$2.45 \cdot v^{-0.60}$	0.41	0.998	Mayhead, 1973
Corsican Pine 4	1.42	-0.49	$1.42 \cdot v^{-0.49}$	0.32	0.991	Mayhead, 1973
Douglas Fir 1	2.34	-0.73	$2.34 \cdot v^{-0.73}$	0.26	0.989	Mayhead, 1973
Douglas Fir 2	2.92	-0.71	$2.92 \cdot v^{-0.71}$	0.35	0.989	Mayhead, 1973
Douglas Fir 3	2.02	-0.66	$2.02 \cdot v^{-0.66}$	0.28	0.989	Mayhead, 1973
Grand Fir	4.50	-0.74	$4.50 \cdot v^{-0.74}$	0.49	0.999	Mayhead, 1973
Lodgepole Pine	1.94	-0.55	$1.94 \cdot v^{-0.55}$	0.37	0.918	Mayhead, 1973
Sitka Spruce 1	1.95	-0.48	$1.95 \cdot v^{-0.48}$	0.46	0.978	Mayhead, 1973
Sitka Spruce 2	2.24	-0.55	$2.24 \cdot v^{-0.55}$	0.47	0.984	Mayhead, 1973
Sitka Spruce 3	2.61	-0.49	$2.61 \cdot v^{-0.49}$	0.61	0.966	Mayhead, 1973
Scots Pine 1	2.06	-0.53	$2.06 \cdot v^{-0.53}$	0.42	0.999	Mayhead, 1973
Scots Pine 2	1.61	-0.48	$1.61 \cdot v^{-0.48}$	0.38	0.991	Mayhead, 1973
Scots Pine 3	1.55	-0.50	$1.55 \cdot v^{-0.50}$	0.34	0.972	Mayhead, 1973
Scots Pine 4*	2.29	-0.72	$2.29 \cdot v^{-0.72}$	0.26	0.972	Mayhead, 1973
Western Hemlock 1	1.59	-0.72	$1.59 \cdot v^{-0.72}$	0.18	0.988	Mayhead, 1973
Western Hemlock 2	1.43	-0.64	$1.43 \cdot v^{-0.64}$	0.21	0.974	Mayhead, 1973
Western Hemlock	2.00	-0.87	$2.00 \cdot v^{-0.87}$	0.55	0.949	Rudnicki et al., 2004
Western Red Cedar	2.86	-0.87	$2.86 \cdot v^{-0.87}$	0.21	0.982	Rudnicki et al., 2004
Lodgepole Pine	2.07	-0.45	$2.07 \cdot v^{-0.45}$	0.53	0.916	Rudnicki et al., 2004

** For this sample, (Mayhead, 1973) determined the drag coefficients in a speed range from 9 to 38m/s.*

The drag coefficients for the coniferous tree species with the dynamic model, taking into account the variable projection area, are shown in Table 12.

TABLE 12 Drag coefficient of the dynamic projection area of fir

FIR	B-VALUE	E-VALUE	C_D	C_D [v=20m/s]	R^2	SOURCE
Western Red Cedar	1.39	-0.29	$1.39 \cdot v^{-0.29}$	0.58	0.976	Rudnicki et al., 2004
Western Hemlock	1.39	-0.14	$1.39 \cdot v^{-0.14}$	0.91	0.949	Rudnicki et al., 2004
Lodgepole Pine	1.36	-0.18	$1.36 \cdot v^{-0.18}$	0.79	0.916	Rudnicki et al., 2004

3.4.2 Drag Coefficients for Deciduous Trees

As above, the results for the analysed drag coefficients for deciduous trees are divided into results for the static model (Table 13) and the dynamic model (Table 14).

TABLE 13 Drag coefficient of the static projection area of deciduous trees

TREE	B-VALUE	E-VALUE	C_D	C_D [20m/s]	R^2	SOURCE
Bigleaf Maple	2.62	-0.76	$2.62 \cdot v^{-0.76}$	0.27	0.974	Vollsinger et al., 2005
Black Cottonwood	2.28	-0.85	$2.28 \cdot v^{-0.85}$	0.18	0.989	Vollsinger et al., 2005
Paper Birch	1.90	-0.82	$1.90 \cdot v^{-0.82}$	0.16	0.997	Vollsinger et al., 2005
Red Alder	2.41	-0.83	$2.41 \cdot v^{-0.83}$	0.20	0.999	Vollsinger et al., 2005
Trembling Aspen	1.80	-0.60	$1.80 \cdot v^{-0.60}$	0.30	0.996	Vollsinger et al., 2005
Red Maple	3.92	-0.63	$3.92 \cdot v^{-0.63}$	0.59	0.998	Kane & Smiley, 2006
White Oak	4.18	-0.76	$4.18 \cdot v^{-0.76}$	0.43	0.998	Kane et al., 2008
Freeman Maple	3.91	-0.68	$3.91 \cdot v^{-0.68}$	0.51	0.999	Kane et al., 2008
Shingle Oak	3.01	-0.62	$3.01 \cdot v^{-0.62}$	0.51	0.996	Kane et al., 2008
Poplar Tree No. 1	1.77	-0.91	$1.77 \cdot v^{-0.91}$	0.12	0.997	Koizumi et al., 2009
Poplar Tree No. 2	1.14	-0.82	$1.14 \cdot v^{-0.82}$	0.10	0.983	Koizumi et al., 2009
Poplar Tree No. 3	1.79	-0.71	$1.79 \cdot v^{-0.71}$	0.21	0.999	Koizumi et al., 2009

TABLE 14 Drag coefficient of the dynamic projection area of deciduous trees

TREE	B-VALUE	E-VALUE	C_D	C_D [20m/s]	R^2	SOURCE
Big leaf Maple	1.21	-0.25	$1.21 \cdot v^{-0.25}$	0.57	0.827	Vollsinger et al., 2005
Black Cottonwood	1.16	-0.26	$1.16 \cdot v^{-0.26}$	0.53	0.979	Vollsinger et al., 2005
Paper Birch	0.92	-0.13	$0.92 \cdot v^{-0.13}$	0.62	0.817	Vollsinger et al., 2005
Red Alder	1.18	-0.29	$1.18 \cdot v^{-0.29}$	0.50	0.968	Vollsinger et al., 2005
Trembling Aspen	1.14	-0.21	$1.14 \cdot v^{-0.21}$	0.61	0.949	Vollsinger et al., 2005

3.4.3 Studies on the Flow Force on Individual Leaves and Clusters of Deciduous Trees

The analysed drag coefficients for clusters are documented in Table 15, while the results for leaves are in Table 16.

TABLE 15 Drag coefficients of clusters of deciduous trees

TREE	B-VALUE	E-VALUE	C_D	C_D [20m/s]	R^2	SOURCE
Black locust	0.16	-0.58	$0.16 \cdot v^{-0.58}$	0.03	0.931	Vogel, 1989
Black walnut	0.49	-0.89	$0.49 \cdot v^{-0.89}$	0.03	0.959	Vogel, 1989
Pignut hickory	1.84	-1.25	$1.84 \cdot v^{-1.25}$	0.04	0.933	Vogel, 1989
Red maple	0.74	-0.89	$0.74 \cdot v^{-0.89}$	0.05	0.979	Vogel, 1989
Tuliptree	1.09	-1.08	$1.09 \cdot v^{-1.08}$	0.04	0.965	Vogel, 1989
White oak	0.15	-0.10	$0.15 \cdot v^{-0.10}$	0.11	0.965	Vogel, 1989
White poplar	0.46	-0.76	$0.46 \cdot v^{-0.76}$	0.05	0.981	Vogel, 1989
Willow oak	0.96	-1.07	$0.96 \cdot v^{-1.07}$	0.04	0.994	Vogel, 1989

TABLE 16 Drag coefficients of leaves of deciduous trees

TREE	B-VALUE	E-VALUE	C_D	C_D [20m/s]	R^2	SOURCE
Tuliptree	3.19	-1.21	$3.19 \cdot v^{-1.21}$	0.08	0.986	Vogel, 1989
Pignut hickory	2.68	-1.27	$2.68 \cdot v^{-1.27}$	0.06	0.955	Vogel, 1989
Red maple	1.42	-0.90	$1.42 \cdot v^{-0.90}$	0.10	0.964	Vogel, 1989
White oak	0.02	1.17	$0.02 \cdot v^{1.17}$	(0.39)	0.996	Vogel, 1989

4 DISCUSSION

The literature search revealed that no detailed studies on wind force dimensioning for overgrown rope façades could be found. For deciduous and coniferous trees, drag coefficients are generated by various experimental studies that have been reflected and compared. The guideline document, "Green Façade Guidelines" (FLL, 2018), however, contains assumption-based reduction factors (drag coefficients) for wind load determination on overgrown rope façades whose physical basis is not clarified.

The studies on deciduous and fir trees often take an approach involving the critical wind speed at which the trees are at risk of toppling. In their calculations, the authors set the drag coefficient at the critical wind speed to a constant value. Depending on the actual location, environment, building shape, and building height, however, different wind speeds arise for the calculation of wind forces on buildings, as shown, for example, in the Swiss standard SIA 261 (SIA 261, 2014) or in the European standard EN 1991-1 to 4 (EN 1991-1-4, 2010). In a corresponding calculation of the resultant forces, as suggested in subsection 3.4, these forces would therefore be underestimated or overestimated at different speeds when using a constant drag coefficient.

The dynamic course of the drag coefficient plays a major role in the calculation of the wind forces of plants on buildings. If the drag coefficient is applied as a function in calculating the resultant forces on overgrown rope façades, the exact drag resistance is calculated at each resultant wind speed.

4.1 EVALUATION OF THE DIFFERENT METHODOLOGIES

The methodology applied in the examined studies varies, although all studies provide established drag coefficients on plants, which makes them comparable if the relevant parameters in Table 10 are taken into account. Since the type of plant (fir tree, deciduous tree, or individual leaves) has an influence on the test results, these parameters are divided and shown separately in section 3 and its subsections. With regard to the methodology, it should be noted that when a pickup truck is driven through a stationary mass of air, a laminar flow around the body is established. This means that the tests by Kane and Smiley (2006) and Kane et al. (2008) are laminar flow profiles, just as it applies for the wind tunnel tests by Mayhead (1973), Rudnicki et al. (2004), and Vollsinger et al. (2005). If these studies are broken down to the plant species, they can be directly compared with each other if the sample-specific parameters according to Table 10 are taken into account. A turbulent flow profile was used by Koizumi et al. (2010) under real conditions and Vogel (1989) in the pipe flow of a fan. Vogel (1989) provides, however, the only study that examined individual blades. Thus, the influence of turbulent pipe flow cannot be identified.

4.2 EVALUATION OF THE DIFFERENT FACTORS

Based on the analysis of the studies in section 3, the following points are discussed, which are assumed to be relevant for determination of the drag coefficients of overgrown rope façades, as well as for the course of the drag coefficient:

1. Size of the samples
2. Flow profile in the environment
3. Projection area
4. Course of the drag coefficient
5. E-value
6. B-value

4.2.1 Size of the Samples

Using a wind tunnel with a larger cross-section, Mayhead (1973) was able to investigate fir samples with heights from 5.8m to 8.5m, whereas Rudnicki et al. (2004) only had access to a smaller wind tunnel cross-section and thus needed to trim the fir samples to a height of 1.9m. In the study by Rudnicki et al. (2004), drag coefficients were obtained at a flow speed of 20m/s for fir species with values of 0.55 (Western Hemlock) and 0.53 (Lodgepole Pine). Whereas in the study by Mayhead (1973) for the same fir species and the same flow speed, drag coefficients were obtained with values of 0.22 (Western Hemlock) and 0.36 (Lodgepole Pine).

Unlike Vollsinger et al. (2005), Kane and Smiley (2006) and Kane et al. (2008) were not subject to any limitations on the size of the samples in their field studies on drag coefficients for deciduous trees. By performing a field test on a moving pickup truck, they were able to test significantly larger

samples. Although identical species of deciduous trees were not investigated in these studies. Kane and Smiley (2006) and Kane et al. (2008) obtained a drag coefficient between 0.43 and 0.59 at 20m/s for red maple, white oak, Freeman maple, and shingle oak. Whereas Vollsinger et al. (2005) obtained significantly smaller drag coefficients for a comparable typology of deciduous trees in the range from 0.16 to 0.30 at 20m/s for big leaf maple, black cottonwood, paper birch, and red alder. However, since Vollsinger et al. (2005) investigated significantly smaller and younger specimens of deciduous trees, the hypothesis is supported by this comparison that older specimens of deciduous trees exhibit greater stiffness and thus less deformation capacity, thereby resulting in higher drag resistances. Older plants therefore absorb considerably more wind energy. It can be assumed that experiments on young plants are not representative, as older plants show significantly higher drag coefficients.

Koizumi et al. (2010) investigated the drag coefficients for standing poplars under natural conditions. In this study, drag coefficients from 0.10 to 0.21 were obtained at 20m/s. These values for the drag coefficients are significantly smaller than what was obtained in the studies of Kane and Smiley (2006) and Kane et al. (2008). In the study of Koizumi et al. (2010), the flow profile is real and not laminar like in the wind channel and pick-up truck studies. This means that a dynamic effect due to the gusty wind flow may be responsible for the lower measured drag coefficients of Koizumi et al. (2010). The dynamic interplay between the plant's deflections in gusts of wind is thus assumed to significantly reduce its resistance. The influence of the flow profile is discussed in section 4.2.2.

4.2.2 Flow Profile in the Environment

The study by Koizumi et al. (2010) is performed under real wind flow conditions. The natural wind spectrum exhibits gusts, for example, which have a significant influence on the results compared to studies in a laminar constant airflow. Koizumi et al. (2010) compared the obtained test results with the test results from the wind tunnel measurements of Mayhead (1973). However, the extent to which the parameters of the different airflow had an influence was not discussed by Koizumi et al. (2010). It is evident that significantly lower flow speeds are obtained due to the real conditions during their measurement compared to laboratory tests. The lower flow speeds in the study by Koizumi et al. (2010) and the resultant uncertainty in the extrapolations could definitely have a further influence on the test results at 20m/s. The analysis shows that for full-grown tree specimens in the natural turbulent airflow, significantly smaller drag coefficients are obtained compared to the wind tunnel studies with laminar airflows. The results of the laminar wind tunnel studies should therefore be on the safe side, as higher drag coefficients result. It is not known whether further influences have an impact on the research results in the tests of Koizumi et al. (2010) in addition to the turbulent wind profile. Therefore, it is not possible to discuss these results in further detail. However, it can be assumed that for the determination of the drag coefficients on plants of overgrown rope façades, a turbulent flow profile must be applied; otherwise, the drag coefficients are overestimated.

4.2.3 Projection Area

The studies of Rudnicki et al. (2004) and Vollsinger et al. (2005) compared the models of the static and dynamic projection areas. Based on the results, it can be concluded that the dynamic model of the drag coefficients exhibits smaller E-values compared to the static model. In the force determination, the assumption of a dynamic projection area A yields, in addition to the dynamic drag

coefficient, is a further dynamic constant in formula (3.4) that makes the calculation more difficult. In contrast, the assumption of a static (fixed) projection area with dynamic drag coefficients has the advantage of only a single dynamic constant reflecting all of the dynamic influences. Therefore, the model approach based on static projection areas appears to be the most suitable one for wind force determination on overgrown rope façades. With exception of Table 12 and Table 14, the studies analysed in section 3 applied static projection areas in the calculation of the drag coefficients, which means that the study results regarding the projection area are comparable.

4.2.4 Course of the Drag Coefficient

According to the reviewed studies, the hypothesis of a potentially decreasing drag coefficient can be confirmed in the wind speed range from 4m/s to 25m/s based on the quality of the functions (R^2) with coefficient of determinations close to 1. The power function can be well fitted to the data points in this speed range. In the lowlands of Switzerland, for example, peak wind speeds occur for gusts in the wind profile of up to 45m/s (SIA 261, 2014). In the speed range from 25 to 45 m/s, no tests were carried out in the studies except for the sample "Scots Pine 4". This means that no conclusion can be drawn in this speed range (with the exception of the singular sample) on the agreement of the power function due to the missing data points. In Fig. 2, the sample "Scots Pine 4" is interpolated. This power function can be well fitted to the data points. Accordingly, it may be concluded that the analysed drag coefficients can be extrapolated by the power function up to a speed of 45m/s.

Mayhead (1973) interpolated the drag coefficients with a 2nd degree polynomial function (cp. formula 2.1). The coefficient of determination is better with a 2nd degree polynomial function. The 2nd degree polynomial function has one degree of freedom more than the power function and can thus be better fitted to the data points. Polynomial functions are applicable only in a certain range and can oscillate outside of this range. Furthermore, the 2nd degree polynomial function does not express any specific E-values, meaning this function does not agree with the model in section 3.2. Due to the constant and the linear term of the polynomial function, this function cannot be directly converted to a power function and can thus not be directly compared to the quadratic speed term of the airflow resistance force formula according to formula (3.4). In order to characterise the drag coefficient of different plants for overgrown rope façades as a function, power functions are thus suitable according to formula (3.3) with B-values and E-values.

4.2.5 E-value

In the study results, the E-values range from -0.43 to -0.87 for firs, -0.60 to -0.85 for deciduous trees, and -0.10 to -1.27 for individual leaves and clusters. For individual leaves and clusters, they exhibit a larger range and differ the most from fir and deciduous trees. The fir and deciduous trees differ only in the lower range and are nearly identical in the upper range with values of -0.87 (fir tree) and -0.85 (deciduous tree).

The E-values determined in section 2.3 are compared in Table 17 with the analysed E-values from the interpolated drag functions. Except for four significant deviations (ΔE-value > 0.2), the comparison confirms the proposed model in section 3.2 with a potential course of the drag coefficients according to formula (3.3). The four deviations of the ΔE-value are identified in the data

of Vogel (1989) for the drag coefficients of leaves. The E-values for deciduous and fir trees exhibit a maximum deviation of 0.09.

TABLE 17 Comparison of E-values from research findings (source) and analysis

SPECIES	E-VALUE SOURCE	E-VALUE ANALYSIS	ΔE-VALUE	DATA SOURCE
Red maple	-0.60	-0.63	0.03	Kane & Smiley, 2006
White Oak	-0.77	-0.76	0.01	Kane et al., 2008
Freeman Maple	-0.77	-0.68	0.09	Kane et al., 2008
Shingle Oak	-0.70	-0.62	0.08	Kane et al., 2008
Scots Pine 4 (Pinus sylvestris)	-0.72	-0.72	0.00	Mayhead, 1973; Vogel, 1984
Black locust leaf	-0.52	-0.58	0.06	Vogel, 1989
Black walnut leaf	-0.76	-0.89	0.13	Vogel, 1989
Pignut hickory leaflet	-0.2	-1.25	1.05	Vogel, 1989
Pignut hickory leaf	-0.78	-1.27	0.49	Vogel, 1989
Red maple leaf	-0.79	-0.90	0.11	Vogel, 1989
Red maple cluster	-0.64	-0.89	0.25	Vogel, 1989
Tuliptree leaf	-1.18	-1.21	0.03	Vogel, 1989
Tuliptree cluster	-0.91	-1.08	0.17	Vogel, 1989
White oak leaf	+0.97	+1.17	0.2	Vogel, 1989
White oak cluster	-0.44	-0.10	0.34	Vogel, 1989
White poplar cluster	-0.60	-0.76	0.16	Vogel, 1989
Willow oak cluster	-1.06	-1.07	0.01	Vogel, 1989

The influence of the E-value on the function is apparent in Figure 3: The two curves are nearly identical for the same B-value and different E-values in the wind speed range from 0 to 2m/s. The curves of the E-values then diverge from one another at the speed range between 2 and 8m/s and, subsequently, continue with a slightly tapering offset with respect to one another. A large E-value thus produces a downward shift of the curve. The influence of the E-value on the drag coefficient is very large, so that when deriving an E-value for climbing plants of overgrown rope façades from analysed data, the correct E-value must be chosen.

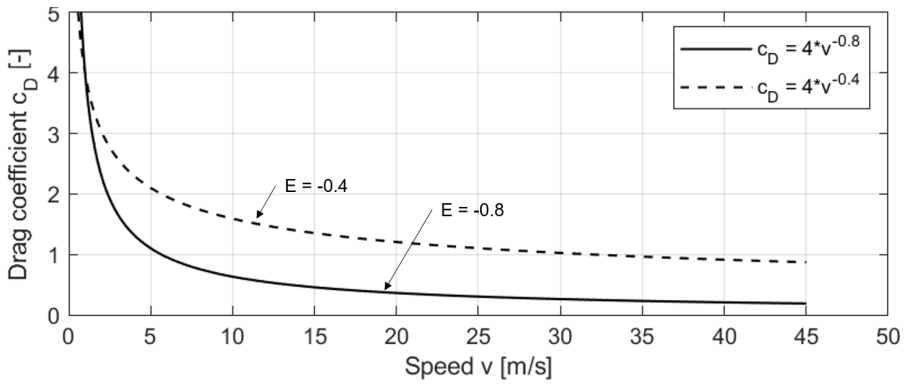

FIG. 3 Shifting of the function for different E-values while maintaining the same B-value

4.2.6 B-value

The B-value is only the constant of the power function before the velocity term (cp. formula (3.3)). Along with the E-value, the B-value has a significant influence on the course of the curve of the drag coefficient (cp. Figure 4). A high B-value causes the function of the drag coefficient to be shifted upward. However, this shift is not constant and it decreases at higher speeds. When deriving a B-value from the analysed data for a drag coefficient for climbing plants of overgrown rope façades, the correct B-value must be chosen.

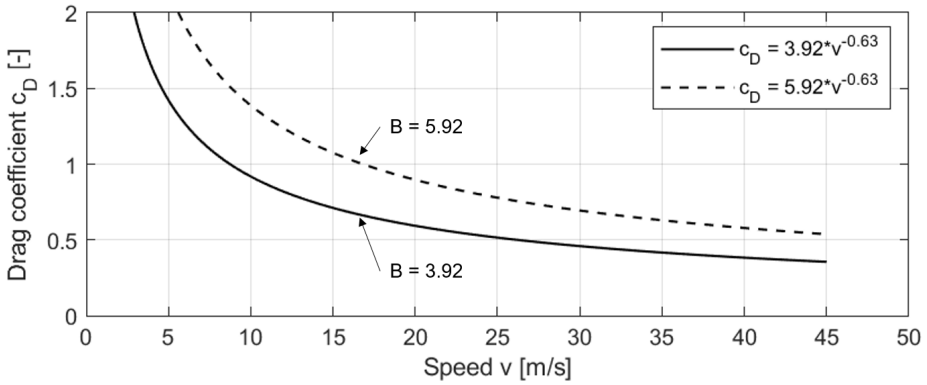

FIG. 4 Shifting of the function for different B-values while maintaining the same E-value

5 HYPOTHESIS FOR NEW DRAG COEFFICIENT DETERMINATION FOR CLIMBING PLANTS ON OVERGROWN ROPE FAÇADES

Since climbing plants do not have needles, they are not analogous to coniferous trees and the studies on the wind forces for coniferous species cannot be applied for wind force determination on overgrown rope façades. Due to the analogy between the leaf shape of climbing plants and the leaf shape of deciduous trees, the study results for deciduous trees for wind force determination could be applied.

However, the morphology of climbing plants does differ from the morphology of deciduous trees. The fact that the morphology has a significant influence on the drag coefficient is demonstrated by the divergent results in studies by Kane and Smiley (2006) and Kane et al. (2008) on larger (and thus older) deciduous tree samples in comparison with the results obtained by Vollsinger et al. (2005) on smaller deciduous tree samples.

In the studies on the drag coefficient for individual leaves of deciduous trees, Vogel (1989) shows that the drag coefficients are mostly less than 0.10 at 20m/s. Contrary to the study results of Kane and Smiley (2006) and Kane et al. (2008) with resultant drag coefficients from 0.43 to 0.59 at 20m/s, individual leaves absorb a small share of the wind force. According to this comparison, the morphology of the tree absorbs a large share of the wind force. An essential role can be attributed to the stiffness of the tree branches.

Comparing the left image in Figure 5 with the right image, an analogy between deciduous trees and climbing plants is apparent: The difference lies in the morphology. Deciduous trees develop a considerably larger crown diameter and bear their own weight as well as the applied loads through their stiff branches, whereas climbing plants are reliant on a host that allows them to climb upwards. They transfer their own weight as well as the applied loads to the host and do not bear these forces on their own.

FIG. 5 Morphology of climbing plants for overgrown rope façades (left) and Morphology of deciduous trees (right)

An analogy between the leaves of deciduous trees and those of climbing plants can also be interpreted from Figure 5. The main difference between these two species lies in the morphology of the wood content. Compared to deciduous trees, climbing plants exhibit a significantly lower wood content. The stiff wooden mass of a deciduous tree is relatively inflexible under flow loading by the wind and is able to align itself in the direction of flow only to a small extent. Due to these inflexible resistance elements, a larger drag coefficient is expected in deciduous trees in comparison with climbing plants - unlike what is, for example, described in the "Green Façade Guidelines" (FLL, 2018). The guidelines base their assumption of higher loads on climbing plants compared to deciduous trees on the denser leaf value associated with the climbing plants. Climbing plants have main shoots on which the leaves grow in a ring pattern, whereas trees have different branches in the tree crown and thus multiple leaves in succession. According to the study by Vogel (1989), the individual leaf generates drag coefficients < 0.1. Denser foliage cannot significantly impact the resultant wind load, because significantly fewer leaves are located in succession in the two-dimensional structures of overgrown rope façades compared to deciduous trees. Multiple leaves in succession in tree crowns add up the individual resistance of the foliage, which means that significantly greater drag resistances can be expected in the airflow for deciduous trees compared to climbing plants. The results of Kane and Smiley (2006) and Kane et al. (2008) with resultant drag coefficients between 0.43 and 0.59 at 20m/s thus provide a reference value for force determination on climbing plants. In order to stay on the safe side (to calculate higher forces in the calculation than actually occur), the highest drag coefficient at 20m/s for the red maple sample in Table 13 is used for wind force determination on overgrown rope façades. The largest B-value (4.18) and smallest E-value (-0.60) in Table 13 are close to the B-value (3.92) and E-value (-0.63) of red maple. This drag coefficient therefore meets the requirements of safe E-values and B-values, making it acceptable for determining the wind forces of climbing plants of overgrown rope façades.

By specifying the drag coefficient as a function and not as a constant at a critical wind speed, the appropriate drag coefficient can be determined for each investigated wind speed on a building. For load determination on overgrown rope façades, the drag coefficient can thus be established based on the curve in Figure 6 at any flow speed.

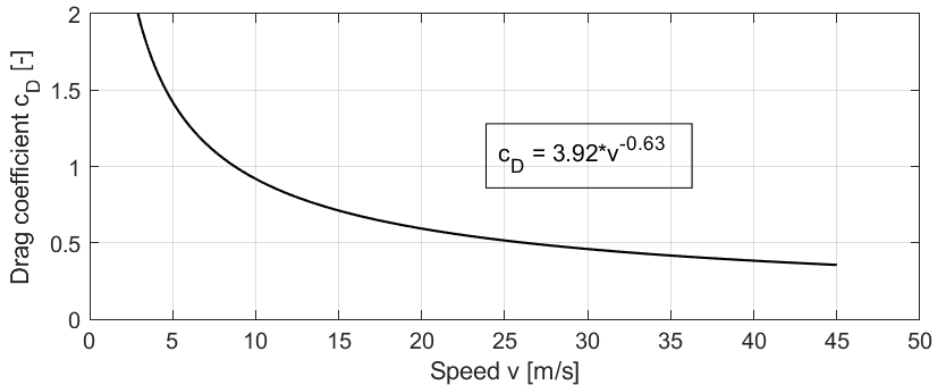

FIG. 6 Reference value of the drag coefficient for overgrown rope façades

The curve in Figure 6 is based on an average value of all drag resistances for the samples. In civil engineering, limit values are derived from the test data by forming a characteristic value from the data points of the sample size for the influence (loads) on the materials as well as for the characteristic resistance values of the materials. However, since the exact test data are not available, it is not possible to determine a characteristic value. The function in Figure 6 thus serves as a rough estimation of the forces and must be considered subject to uncertainties.

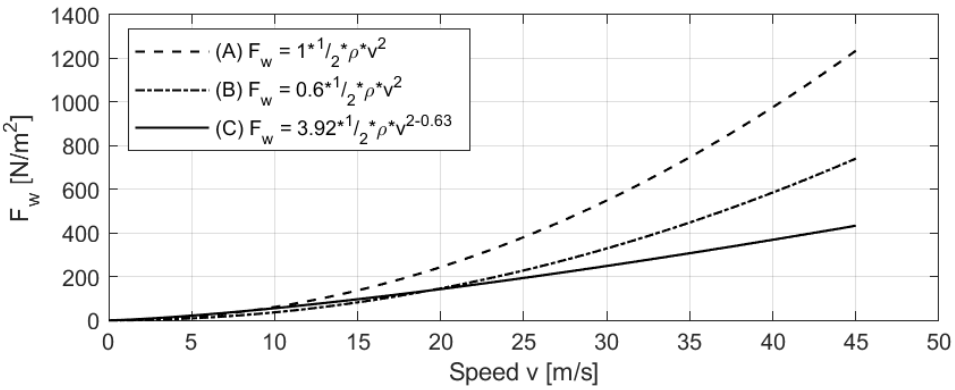

FIG. 7 Comparison of the different curves A (top), B (middle) and C (bottom)

Figure 7 shows the potential that lies in the determination of the exact drag coefficients for calculation of the wind forces for overgrown rope façades. The top curve (A) is based on the full wind forces with a drag coefficient of 1. At 45m/s, an airflow resistance of 1235N/m^2 is obtained. The middle curve (B) is based on diminished wind forces with a constant drag coefficient according to (FLL, 2018) of 0.6 for the "medium" load class. At 45m/s, an airflow resistance of 740N/m^2 is obtained. The bottom curve (C) is based on the dynamic drag coefficient (cp. Figure 6) that is defined versus speed and expressed as a function. At 45m/s, an airflow resistance of 400N/m^2 is obtained,

representing 1/3 of curve (A). In order not to overestimate the wind loads on the climbing plants of overgrown rope façades, it is essential to determine the drag coefficients by means of a power function. The assumption of full wind loads (A) or the estimation of the drag coefficients by constants (B) (not as functions over the speed range) leads to high loads at the wind speeds occurring on the building and therefore to higher material wear and higher costs.

6 CONCLUSION

In the review of the identified studies, different methods are analysed for determination of the flow forces on coniferous and deciduous trees, as well as on individual leaf types. Through the subsequent analysis and evaluation of the data, it can be assumed that the study results of Kane and Smiley (2006) can be applied to obtain a rough estimation of the wind forces on overgrown rope façades. The analogy between deciduous trees and climbing plants is drawn due to the similar leaf shape. However, deciduous trees differ from climbing plants in terms of the morphology. Due to the rigid branches of deciduous trees, a greater wind force is presumed on deciduous trees, whereby the drag coefficients of deciduous trees form an upper limit. The Red maple plant species from the results of the study by Kane and Smiley (2006) achieved the highest drag coefficient at 20m/s. This result is applied as the upper limit for a drag coefficient of climbing plants.

The analysis and verification of the course of the drag coefficient based on a power function represent an important result. By specifying the drag coefficient as a function, the drag coefficient and thus the wind forces may be determined at any given wind speed in the design of overgrown rope façades.

The drag coefficient suggestion determined in this paper is based on various assumptions and serves as an initial rough approximation for determination of the wind forces. The hypothesis that the different morphology of climbing plants compared to deciduous trees leads to smaller drag coefficients must be confirmed in a further study. Since no studies are found concerning the wind force on climbing plants, tests are necessary to determine plant-specific parameters for climbing plants for use in wind force determination. The tests must be carried out in an airflow that simulates the natural airflow resulting from wind.

In order to further investigate the calculation parameters for the wind force on overgrown rope façades, a further study is planned that will focus on the measurement of the drag resistances on five selected climbing plants in a turbulent wind tunnel, followed by determination of the drag coefficients to the statistical characteristic value.

Acknowledgement

This work was carried out in the course of an in-depth study for a master's programme. The main author would like to thank Lucerne University of Applied Sciences and Arts (Lucerne School of Engineering and Architecture) for its support in elaborating the results of this paper.

References

Alexandri, E. & Jones, P. (2008). Temperature decreases in an urban canyon due to green walls and green roofs in diverse climates. *Building and Environment*, *43*(4), 480–493. doi: 10.1016/j.buildenv.2006.10.055

Djedjig, R., Bozonnet, E., & Belarbi, R. (2015). Experimental study of the urban microclimate mitigation potential of green roofs and green walls in street canyons. *International Journal of Low-Carbon Technologies*, *10*(1), 34–44. doi: 10.1093/ijlct/ctt019

EN 1991-1-4. (2010). Eurocode 1: Actions on structures - Part 1-4: General actions - Wind actions. [Standard].

FLL. (2018). *Fassadenbegrünungsrichtlinien-Richtlinie für die Planung, Ausführung und Pflege von Wand- und Fassadenbegrünungen* [Façade greening guidelines - Guideline for the planning, execution and maintenance of wall and façade greenings]. [Guideline]. Bonn.

Gartland, L. M. (2012). *Heat Islands:* Understanding and Mitigating Heat in Urban Areas. Routledge. doi: 10.4324/9781849771559

Kane, B., Pavlis, M., Harris, J. R., & Seiler, J. (2008). Crown reconfiguration and trunk stress in deciduous trees. *Canadian Journal of Forest Research*, *38*, 1275–1289. doi: 10.1139/X07-225

Kane, B. & Smiley, E. T. (2006). Drag coefficients and crown area estimation of red maple. *Canadian Journal of Forest Research*, *36*(8), 1951–1958. doi: 10.1139/x06-086

Koizumi, A., Motoyama, J., Sawata, K., Sasaki, Y., & Hirai, T. (2010). Evaluation of drag coefficients of poplar-tree crowns by a field test method. *Journal of Wood Science*, *56*(3), 189–193. doi: 10.1007/s10086-009-1091-8

Kolokotsa, D., Santamouris, M., & Zerefos, S. C. (2013). Green and cool roofs' urban heat island mitigation potential in European climates for office buildings under free floating conditions. *Solar Energy*, *95*, 118–130. doi: 10.1016/j.solener.2013.06.001

Leal Filho, W., Echevarria Icaza, L., Emanche, V. O., & Quasem Al-Amin, A. (2017). An Evidence-Based Review of Impacts, Strategies and Tools to Mitigate Urban Heat Islands. *International Journal of Environmental Research and Public Health*, *14*(12). doi: 10.3390/ijerph14121600

Mayhead, G. J. (1973). Some drag coefficients for british forest trees derived from wind tunnel studies. *Agricultural Meteorology*, *12*, 123–130. doi: 10.1016/0002-1571(73)90013-7

Meskouris, K., Butenweg, C., Hake, E., & Holler, S. (2012). *Baustatik in Beispielen* (2nd ed.) [Structural analysis in examples]. Berlin Heidelberg: Springer-Verlag. doi: 10.1007/978-3-642-23530-6

Mohajerani, A., Bakaric, J., Jeffrey-Bailey, T., & Mohajerani, A. (2018). The Urban Heat Island Effect, its Causes, and Mitigation, with Reference to the Thermal Properties of Asphalt Concrete. *Journal of Environmental Management*, *197*, 522–538. doi:10.1016/j.jenvman.2017.03.095

Pfoser, N. (2016). *Fassade und Pflanze. Potenziale einer neuen Fassadengestaltung* [Façade and plant. Potentials of a new façade design]. [Dissertation]. Technische Universität Darmstadt, https://tuprints.ulb.tu-darmstadt.de/id/eprint/5587

Pfoser, N. (2018). *Vertikale Begrünung* [Vertical greening]. Stuttgart: Verlag Eugen Ulmer. ISBN 978-3-8186-0088-4

Rudnicki, M., Mitchell, S. J., & Novak, M. D. (2004). Wind tunnel measurements of crown streamlining and drag relationships for three conifer species. *Canadian Journal of Forest Research*, *34*(3), 666–676. doi: 10.1139/x03-233

Santamouris, M., Papanikolaou, N., Livada, I., Koronakis, I., Georgakis, C., Argiriou, A., & Assimakopoulos, D. N. (2001). On the impact of urban climate on the energy consumption of buildings. *Solar Energy*, *70*(3), 201–216. doi: 10.1016/S0038-092X(00)00095-5

SIA 261. (2014). *Einwirkungen auf Tragwerke* [Actions on supporting structures]. [Standard]. Switzerland

Vogel, S. (1984). Drag and Flexibility in Sessile Organisms. *American Zoologist*, *24*(1), 37–44. JSTOR. doi: 10.1093/icb/24.1.37

Vogel, S. (1989). Drag and Reconfiguration of Broad Leaves in High Winds. *Journal of Experimental Botany*, *40*(8), 941–948. doi: 10.1093/jxb/40.8.941

Vollsinger, S., Mitchell, S., Byrne, K., Novak, M., & Rudnicki, M. (2005). Wind tunnel measurements of crown streamlining and drag relationships for several hardwood species. *Canadian Journal of Forest Research*, *35*, 1238–1249. doi: 10.1139/x05-051